Photoconductivity Measurements of X-ray Absorption Fine Structures in Liquids in the Soft X-ray Region: Si and Cl K-edge

T.K. SHAM, R.A. HOLROYD[*], J.-Z. XIONG, X.H. FENG and B.X. YANG[b]

Department of Chemistry, University of Western Ontario, London N6A 5B7, Canada
[*]Chemistry Department, Brookhaven National Laboratory, Upton, NY 11973, U.S.A.
[b]CARS, University of Chicago, Chicago, IL 60637, U.S.A.

Photoconductivity measurements of X-ray absorption fine structures (XAFS) at the Si and Cl K-edge have been carried out in a liquid cell for $(CH_3)_4Si$, $[(CH_3)_3Si]_4Si$ and CCl_4, either as a pure liquid or in a 2,2,4- trimethylpentane solution. It is found that for the pure liquids and their concentrated hydrocarbon solutions, all K-edge XAFS spectra are inverted as expected under the condition of total absorption. A sharp conductivity dip is also observed in CCl_4 at the Cl K-edge. The concentration dependence of the XAFS spectrum of CCl_4 is reported in some details. These results are discussed in terms of the soft X-ray induced ion yields of the solute and solvent molecules in liquids.
KEYWORDS: soft X-ray, photoconductivity of liquids, XAFS

§1. Introduction

We have been interested in direct-current (DC) measurements of synchrotron radiation induced ion yield of hydrocarbon liquids (hexane and iso-octane for example) and solutions of organometallic compounds in them for some time[1-6]. The objectives of these studies are to obtain the heretofore little known information on the free ion yields for liquid hydrocarbon in the X-ray photon energy range previously inaccessible with conventional sources; this information is relevant to radiation chemistry studies and can in turn be used for the design and implementation of liquid detectors[7]; one of such applications is to record the X-ray absorption fine structures (XAFS) of an element in hydrocarbon solutions below and above an absorption edge[3,6]. Experiments that have been carried out so far are in the 4-30 keV photon energy range[6,8]. Here, we extend our study to lower energies, from 4 keV to just below the Si K-edge (1.8 keV).

Let us for the moment review the current status of the technique. First, like other yield methods, conductivity measurement assumes that the ion yield in liquids generally relates to the absorption coefficient of the liquid across the absorption edge of interest. Second, the free ion yield (G value) for hydrocarbon liquids plays an important role in the measurement and is of the order of 0.1 to 0.4 (ions/100eV absorbed) for X-rays with energies from 4-30 keV respectively, and it decreases as the photon energy decreases[2,6,8]. This trend can be interpreted on the basis of a track model[9] in which the ion yield is related to the gradient of energy loss of the energetic electrons (dE/dx) created by the X-ray absorption process along the ionization track. These energetic electrons are primarily responsible for the production of ion pairs that are eventually detected, the larger the gradient the smaller the yield[8]. The ion yield is expected to decrease further as the photon energy decreases to below 4 keV. Third, when a solute is present in a liquid hydrocarbon, the total ion yield of the solution across an absorption edge does not always behave like a normal absorption edge at photon energies across the edge of interest. In fact, more often than not, the ion yield spectrum across the absorption edge of the solute exhibits features distinctly different from the normal absorption edge, depending on the concentration of the solute and other experimental parameters (such as photon flux, total sample thickness and electric field). In general, when the sample is thin and the solute concentration is low (the absorbing atom only constitutes a small fraction of the sample), the ion yield will exhibit a positive edge jump as expected from an absorption spectrum while with thick samples at high concentrations, the ion yield is always inverted at the edge (negative edge jump) and at a narrow region of intermediate concentrations and thickness it shows the details of the inversion process. It is in fact the total thickness of the sample as well as the concentration of the individual elements in the solution that are responsible for the shape of the conductivity XAFS spectrum. This behaviour has been reported in the study of tetramethyltin in TMP at the Sn K- and L-edges[5,6] and has been interpreted in terms of the competitive absorption for total photon flux between the solute and solvent[5,6,8]. This technique has also been suggested as an useful alternative in XAFS measurements of thick (concentrated) samples which absorb all the incoming photons[4]. This technique is particularly relevant for measurements in the soft x-ray range such as the K-edge of Si, P, S and Cl because at these energies, the samples are always too thick (one absorption length for Si at the Si K-edge is ~ 1.3 μm) and it is almost impossible to prepare liquid sample cells of one absorption length[10]. We report here some recent XAFS measurements of liquids at the Si and Cl K-edge using this ion yield (conductivity) technique with "thick cells". The results substantiate that the conductivity technique is indeed a good alternative for K-edge XAFS measurements of these elements in the liquid state. The solutes of interest are $(CH_3)_4Si$ (TMS), $[(CH_3)_3Si]_4Si$ (henceforth denoted SiSi4), and CCl_4, all spherical molecules and the solvent is 2,2,4- trimethylpentane (TMP).

§2. Experiment

X-ray absorption measurements were carried out at

the UHV compatible double crystal beamline of the Canadian Synchrotron Radiation Facility (CSRF) at the Synchrotron Radiation Center (SRC), University of Wisconsin–Madison. This beamline is equipped with a InSb(111) crystal monochromator and a post–focusing mirror with an upper cut–off energy of ~3.7 keV[10]. The crystal angle scan of this beamline has extremely good mechanical stability over the entire energy range and has no higher order radiation problems[11]. The monochromatic photon beam is at a fixed–exit position during a scan. To achieve this, the position of the beam is monitored by a two–wire feed–back system with the wires placed above and below the beam. The incoming photon flux is monitored with a in–line nitrogen ionization chamber calibrated at a pressure of 1.15 torr^8, so that absolute photon flux can be obtained. Photon energy was calibrated at the Si K–edge of a Si(111) crystal at 1839 eV at the beginning of each fill. No further calibration was attempted at the Cl K–edge.

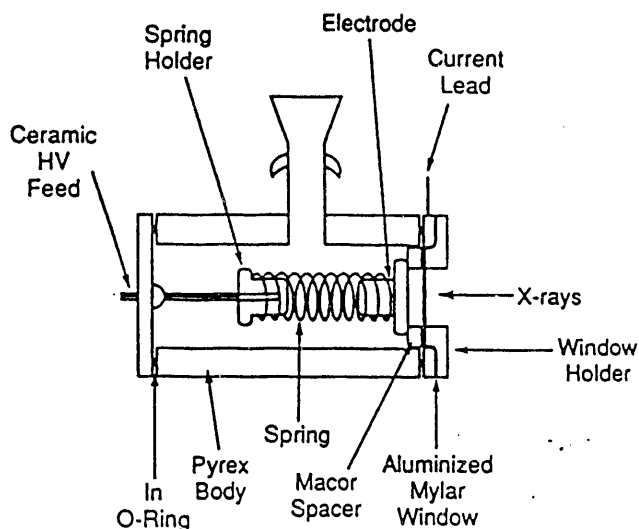The liquid cell used in this study is shown in Fig.1.

Fig.1 Schematic drawing of the liquid cell used in the experiment.

The electrodes are parallel to each other and perpendicular to the incoming photon beam. The first electrode through which the beam enters is an aluminized mylar window, the Al film (150μg/cm^2) serves as a current collecting electrode. The high voltage electrode is held by a thin macor washer. The electrode separation is 0.069 cm which is thin enough to allow a reasonable high voltage to be applied across the electrodes to ensure near–unity cell efficiency, yet it is thick enough to provide more than several absorption lengths of the liquid under study. Therefore this cell is suitable for current measurements under the condition of total absorption.

The cell is placed in a small aluminium chamber positioned at the photon exiting beam–port which is equipped with a 25μ Be window. The Be window separates the UHV environment from the atmosphere. A He path at atmospheric pressure between the Be window and the first electrode (2 cm gap) is provided by passing He through the cell holder assembly at a very low float

rate. Under these conditions, the dark current of the cell at 700 V (1000 V/cm, a typical voltage used in the measurement) is less than 10 pA. In most of the measurements, the photon flux was attenuated with mylar films so that the cell current is of the order of 0.1 nA by desire to minimize recombination of ions. Under these conditions the cell detection efficiency is approximately unity.

All the liquids (99.9 % purity) used in this study were obtained commercially. Each liquid was further purified and characterized^8 to ensure that there is no impurity present in any significant amount that would interfere with the measurement. The solid sample ([(CH$_3$)$_3$Si]$_4$Si) was prepared and characterized in the laboratory according to published methods and was purified by sublimation prior to the experiment. TMS and CCl$_4$ were studied as pure liquids and as a series of TMP solutions while only a dilute solution of SiSi4 was studied.

§3. Results and Discussion

Fig. 2 shows the monotonic increase of the G value of TMP as a function of photon energy measured at 7.2 kV/cm. In terms of photons, the yield is 2.2 and 3.9 ion per photon absorbed at the energies corresponding to Si (1840 eV) and Cl (2813 eV) K–edge respectively. These values bear some significance in the appearance of the conductivity XAFS as it will become clear below.
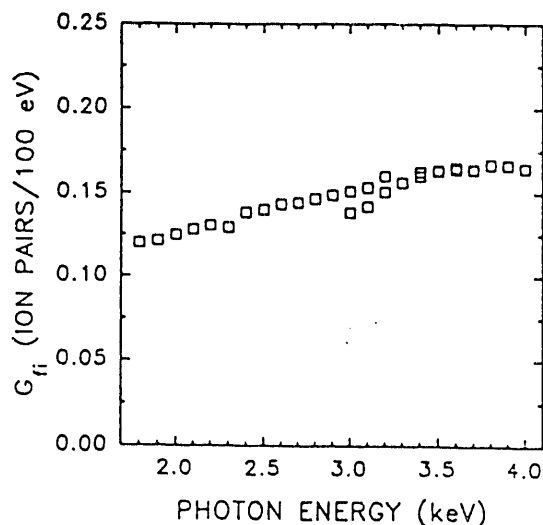

Fig.2 G value (ion/100 eV absorbed) for TMP from 1.8 to 4 keV photon energy at 7.2 kV/cm.

Fig. 3 shows the conductivity yield of TMS in TMP as a function of concentration. The upper panel compares the near–edge structure of gaseous (absorption) and liquid TMS (conductivity); the lower panel shows the concentration dependence of the conductivity measurements of TMS in TMP, with the pure liquid showing the biggest negative resonance (dip at ~1845 eV) which becomes smaller upon dilution (by volume) to 50%, 25%, and 10%. The 25% sample already exhibits a nearly flat region. The 10% sample is indistinguishable from the pure solvent probably because the concentration of Si is too
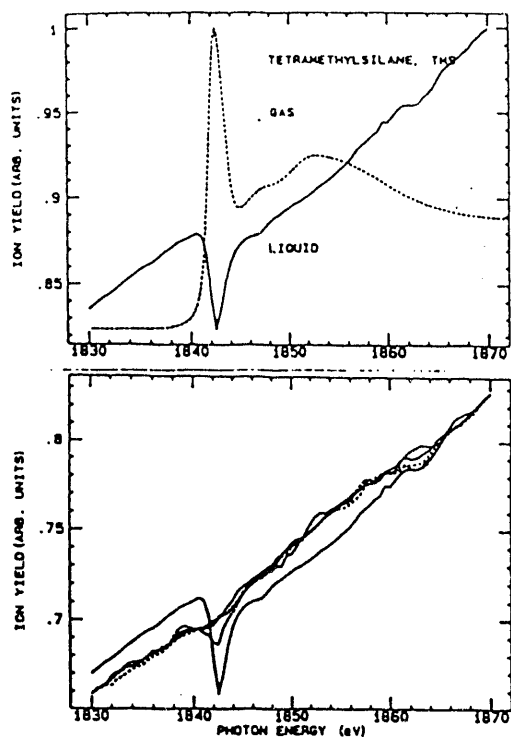
Fig. 3. Upper panel: comparison of gas phase near edge structure with that of liquid TMS (conductivity); lower panel: XAFS of TMS in TMP at concentrations of 100%, 50%, 25% ,10% and 0% by volume.

low (since the molecule itself contains 4 carbon atoms, Si is already diluted in the molecule).

The sharp resonance at ~1845 eV in Fig.2 arises from dipole transitions from the Si 1s to molecular orbitals of a_1 and t_2 symmetry. These are localized transitions with transition energies below the ionization threshold. It should be noted that in molecular systems, the edge structure generally consists of features arising from bound (core) to bound (valence) transitions, bound to quasi-bound transitions (shape resonances) and bound to continuum transitions. The bound to bound transitions often feature strong whitelines from atomic to molecular orbital transitions and some weak Rydberg states at energies below the ionization threshold[12,13]. Therefore, the edge threshold (often taken as the point of inflection of the rising edge) is not the same as the ionization threshold in molecular systems. In the case of TMS, the ionization threshold is higher than that of the intense resonance by ~ 5 eV. The subtle difference between the bound to bound transition and the transitions above the ionization threshold relevant to our discussion is the way the excited molecule dissipates the absorbed energy in the subsequent decay processes. The excited state produced by a localized transition differs from the ionized state produced by photons with energy above the continuum (ionization threshold) by virtue of the presence of the extra electron in the previously unoccupied orbital in the vicinity of the molecule (this electron would become a low energy photoelectron for transitions above the threshold); this electron can act as a spectator electron or it can participate in the Auger process. The excited molecule, upon Auger decay, can be found in either a two-hole, one valence electron or a one-hole state as to be distinguished from a two-hole state in the ionized molecule[14]. This

difference would lead to different fragmentation patterns which often distribute more energy to the fragmented ions and neutrals than it would have in the case of an ionized molecule[15,16]. In either event, these processes would be less effective in producing energetic electrons hence ions in the solvent then the absorption processes below the edge.

Fig.4 shows the concentration dependence of the conductivity XAFS at the near edge region of the Cl K-edge for CCl_4 in TMP. Again, we can clearly see the inversion of the Cl K-edge in pure CCl_4 which shows a sharp resonance with a 23% dip in ion yield relative to the yield just below the edge. The dip becomes smaller as CCl_4 is further diluted in TMP. At as low as 1.69% concentration however, the spectrum still exhibits a dip in the sharp resonance region. This observation is in general agreement with previous observations in that the edge jump is always inverted with thick cells (total absorption). In shallower edges or edges of low Z elements of which the absorption edge falls in the soft X-ray region, the desired concentration and cell thickness with which the liquid sample may exhibit an positive edge jump is almost impossiblte to obtain experimentally because it is very difficult to prepare samples with one absorption length at these photon energies.

The experimental observations can now be understood on the basis of the following: (a) In these measurements, practically, all the photons incident upon the sample are absorbed, therefore the fraction of photons absorbed by the solute and solvent will change and may change abruptly
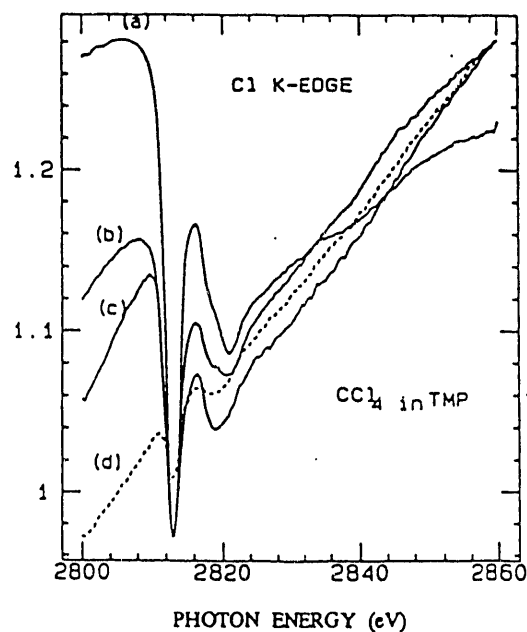

Fig.4 Conductivity XAFS of CCl_4 in TMP: (a) 100%, (b) 48%, (c) 6.8% and (d)1.6% by volume.

at the edge threshold, (b) energetic electrons (which are created by photoionization) are primarily responsible for the X-ray absorption induced conductivity through energy loss (with a gradient dE/dx) in the liquid along the ionization track, and (c) the absorption (per photon absorbed) above the edge is generally less effective in producing ions than that below the edge; this is because the new excitation channels created at and above the edge

produce relatively low energy photoelectron. Most of the energy are carried by the Auger electrons which are certainly less energetic than the shallower shell photoelectrons that would have been created in the absence of the K-edge channels. For a bound to bound dipole transition above the edge but below the ionization threshold (such as the most intense resonance seen in TMS and CCl$_4$, a significant fraction of the energy may be converted to the kinetic energy of molecular fragments according to a specific de-excitation channel[15] leaving behind less-energetic electrons to ionize the solvent. In addition, a small portion of the excitation energy will decay via fluorescence of which a fraction may escape the system without producing any ionization. This process becomes more important with increasing atomic number.

The edge jump behaviour can now be discussed phenomenologically based on the above considerations. It is convenient to monitor the edge behaviour using the ratio of the ion yield signal, R, above and below the edge (above the edge refers to all new channels originated from the Si or Cl 1s in this analysis, bound to bound and bound to continuum alike). R > 1 for positive edge and R < 1 for negative edge. R can be expressed as[6]

$$R = \frac{(1-\exp[-\mu^a t])}{(1-\exp[-\mu^b t])} \times \frac{[f(c)^a Y(c)^a + f(S)^a Y(S)^a]}{[f(c)^b Y(c)^b + f(S)^b Y(S)^b]} \quad (1)$$

where the μ's are the absorption coefficients above and below the edge (denoted with a and b respectively), and the f's and Y's are the fraction of the photons absorbed and the yields of the hydrocarbon solvent and the liquid solute (denoted c and S respectively). Since the μt's are very large in these measurements, the first term is always unity and R is determined entirely by the ratio of the second term. Under this total absorption condition, f(c)Y(c) and Y(S) below the edge are greater than those above the edge while f(S) is larger above the edge. This is because the ion yield for the hydrocarbon liquid is significantly greater than that of the solute which is often composed of elements heavier than carbon and itself often contains carbon. For example, the photoelectrons produced in hydrocarbon come primarily from the K-edge channel which yields energetic electrons with kinetic energy of 1544 eV for X-ray energy of 1830 eV (just below the Si K-edge). Si and Cl will absorb a bigger fraction of photons above the edge but the electrons produced will be less energetic, therefore the ion yield per energy unit absorbed is smaller.

Fig. 5 shows the ion yield of pure CCl$_4$ liquid at 3.6 kV/cm where Cl absorbs 95% of the photons below the Cl K-edge and 99% above. In comparison with Fig. 2, it is apparent that the ion yield of TMP is a factor of 1.9 of that of CCl$_4$ at photon energies just below the Cl K-edge (2800 eV) and a factor of 2.3 just above (2830 eV) when the results are normalized to the same field strength (10kV/cm)[9]. The yield gets worse for stronger absorptions above the Cl K-edge. The Auger electrons which carry most of the energy in the de-excitation process (fluorescence yield is small at these levels) are less energetic than the L-shell and valence photoelectrons in total absorption, therefore they would produce a smaller number of ionization events in the liquid than what would have been below the edge.
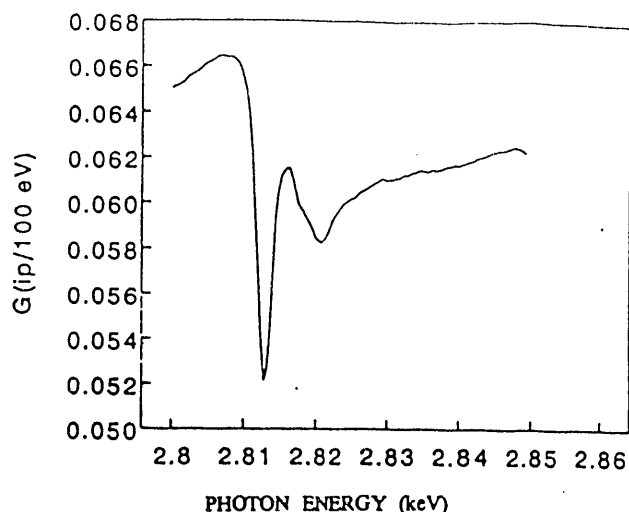

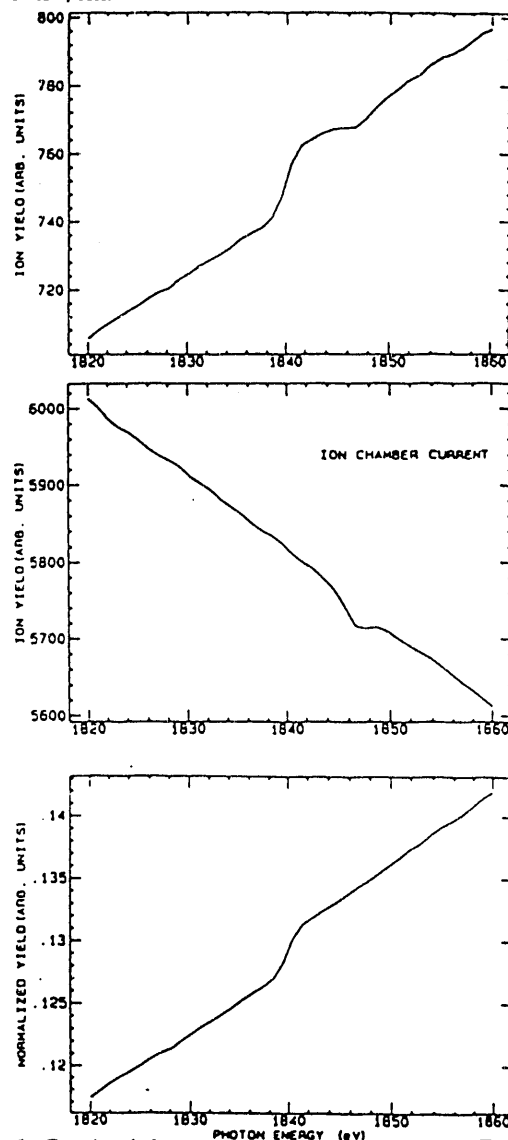Fig. 5. G value of pure CCl$_4$ liquid across the Cl K-edge at 3.5 kV/cm.

Fig. 6. Conductivity spectrum of SiSi4 in TMP; from top to bottom: ion Yield, I$_0$ and ion yield normalized to I$_0$.

It is quite apparent from equation (1) that in the case of CCl$_4$, the R value would be approaching unity upon dilution in TMP from a fractional number. R for the pure

liquid at 10 kV/cm is 0.073/0.086 = 0.85^9. There is no chance for a changeover from negative to positive unless the sample becomes optically thin so that some of the X-rays will transmit, then the first term in equation (1) will become greater than unity.

The trends shown in Figs. 3 and 4 can now be understood in terms of this competitive absorption model based on the difference in ion yields between solutes and solvents and above and below the edge of the Si and Cl K-edge respectively. If all the photons are absorbed, according to equation (1), no positive edge will be observed. Only when the cell is thin, then a positive jump in the conductivity spectrum may be observed if the cell is not totally black. This has not been observed in both TMS and CCl$_4$ TMP solutions at the concentrations we have investigated, presumably the cells are totally black at these concentrations (one absorption length for TMP is ~ 40 micron). Only in the case of [(CH$_3$)$_3$Si]$_4$Si in TMP, a preliminary study of the Si K-edge conductivity XAFS of a dilute solution in TMP seems to show a small positive edge jump (a few percent) without any structure. This is shown in Fig.6. The main difference between SiSi4 and TMS is the local Si density in the molecule (the Si to C ratio is 1 to 2.4 in the former and 1 to 4 in the latter). The relevance of this, if any, is not clear at present. Systematic measurement and analysis is needed to quantify this observations.

§4. Summary and Conclusion

We have reported conductivity XAFS measurements at the Si and Cl K-edge for compounds as a pure liquid and dissolved in TMP. The results clearly show that the technique is a good alternative to transmission measurements which cannot be easily performed for low Z element liquids. The ion yield of hydrocarbon liquids in the soft X-ray region of 1.8 to 4 keV has been used to interpret the observation of the negative edge dip. It is shown that the competitive absorption model is also valid for the interpretation of conductivity XAFS from 1.8 to 4 keV. It should also be noted that this discussion will have some relevance to other yield techniques such as luminescence yield XAFS.

References

1. T.K. Sham and S.M. Heald, J. Amer. Soc. 105, 5142(1983).
2. R.A. Holroyd and T.K. Sham, J. Phys. Chem. 89, 2909(1985).
3. T.K. Sham, R.A. Holroyd and R.C. Munoz, Nucl. Inst. Meth. A 249, 530(1986).
4. T.K. Sham in "Application of Synchrotron Radiation in Chemistry and Biology I" edited by E. Mandelkow, Springer Verlag, Berlin, p 81,(1988).
5. T.K. Sham and R.A. Holroyd, Phys. Rev. B 39, 8257(1989).
6. T.K. Sham, P. Kristof and R.A Holroyd, Rev. Sci. Instr. 63, 1198(1992).
7. BNL Report No. 52244, edited by B. Yu and V. Radeka (1990).
8. R.A. Holroyd, T.K. Sham, B.X. Yang and X.H. Feng, J. Phys. Chem. in press.
9. G. Jaffe, Annalen der Physik 42, 303(1913).
10. See for example B.L. Henke, P. Lee, T.J. Tanaka, R.L. Shimabukuro and B.K. Fujikawa, :Low Energy X-Ray Interaction Coefficients: Photoabsorption, Scattering and Reflection" At. Data Nucl. Data Table 27,1(1982).
11. B.X. Yang, F.H. Middleton, B.G. Olsson, G.M. Bancroft, J.M. Chen, T.K. Sham, K.H. Tan and D.J.Wallace. Nucl. Instr. Meth. A, 316, 422(1992).
12. T.K. Sham, Acct. Chem. Res. 19,99(1988).
13. J. Stohr "Near Edge X-Ray Absorption Fine Structures" Spriger Verlag (1992).
14. W. Eberhardt, T.K. Sham, R. Carr, S. Krummacher, M. Strongin, S.L. Weng and D. Wesner, Phys. Rev. Lett. 50, 1038(1983), and W. Eberhardt and T.K. Sham, SPIE 447, 143(1984).
15. D.M. Hanson, Adv. Chem. Phys. 77, 1 Wiley, N.Y. (1990).
16. T.K. Sham, B.X. Yang, J. Kirz and J.S. Tse, Phys. Rev A. 40, 652(1989).

END

DATE
FILMED
5/05/93